AMERICAN SOCIETY FOR MICROBIOLOGY | Applied and Environmental Microbiology®

PHYSIOLOGY

The Oligosaccharyltransferase AglB Supports Surface-Associated Growth and Iron Oxidation in *Methanococcus maripaludis*

Matthew P. Holten,[a] Dallas R. Fonseca,[a] Kyle C. Costa[a]

[a]Department of Plant and Microbial Biology, University of Minnesota, Twin Cities, St. Paul, Minnesota, USA

ABSTRACT Most microbial organisms grow as surface-attached communities known as biofilms. However, the mechanisms whereby methanogenic archaea grow attached to surfaces have remained understudied. Here, we show that the oligosaccharyltransferase AglB is essential for growth of *Methanococcus maripaludis* strain JJ on glass or metal surfaces. AglB glycosylates several cellular structures, such as pili, archaella, and the cell surface layer (S-layer). We show that the S-layer of strain JJ, but not strain S2, is a glycoprotein, that only strain JJ was capable of growth on surfaces, and that deletion of *aglB* blocked S-layer glycosylation and abolished surface-associated growth. A strain JJ mutant lacking structural components of the type IV-like pilus did not have a growth defect under any conditions tested, while a mutant lacking the preflagellin peptidase (Δ*flaK*) was defective for surface growth only when formate was provided as the sole electron donor. Finally, for strains that are capable of Fe^0 oxidation, we show that deletion of *aglB* decreases the rate of anaerobic Fe^0 oxidation, presumably due to decreased association of biomass with the Fe^0 surface. Together, these data provide an initial characterization of surface-associated growth in a member of the methanogenic archaea.

IMPORTANCE Methanogenic archaea are responsible for producing the majority of methane on Earth and catalyze the terminal reactions in the degradation of organic matter in anoxic environments. Methanogens often grow as biofilms associated with surfaces or partner organisms; however, the molecular details of surface-associated growth remain uncharacterized. We have found evidence that glycosylation of the cell surface layer is essential for growth of *M. maripaludis* on surfaces and can enhance rates of anaerobic iron corrosion. These results provide insight into the physiology of surface-associated methanogenic organisms and highlight the importance of surface association for anaerobic iron corrosion.

KEYWORDS *Archaea*, *Methanococcus*, N-linked glycosylation, biofilm, iron oxidation

A nearly ubiquitous feature of microbial life is the ability to grow as a surface-associated community known as a biofilm (1). While biofilms are well studied in many members of the *Bacteria*, work on understanding the mechanisms underlying biofilm attachment and maturation in the *Archaea* has focused primarily on *Haloferax* spp. and *Sulfolobus* spp. as model organisms (2, 3). In these organisms, extracellular appendages such as pili and archaella (archaeal flagella) are essential for initial surface attachment (2, 3), and glycosylation of these appendages plays an important role in biofilm formation (4). Additionally, *Sulfolobus solfataricus* displays strain-specific biofilm phenotypes on different surfaces, and extracellular polymeric substances (EPS) were found to be significantly different between strains (5). These differences were attributed to a 47-gene region carrying genes predicted to function in sugar and lipid metabolism on the genome of one strain, suggesting altered EPS production and composition.

Citation Holten MP, Fonseca DR, Costa KC. 2021. The oligosaccharyltransferase AglB supports surface-associated growth and iron oxidation in *Methanococcus maripaludis*. Appl Environ Microbiol 87:e00995-21. https://doi.org/10.1128/AEM.00995-21.

Editor Haruyuki Atomi, Kyoto University

Address correspondence to Kyle C. Costa, kcosta@umn.edu.

Received 20 May 2021
Accepted 6 June 2021
Accepted manuscript posted online 16 June 2021
Published 11 August 2021

In addition to *Haloferax* spp. and *Sulfolobus* spp., several members of the methanogenic archaea grow as surface-attached communities. These include *Methanosarcina mazei* strain Gö1, methanogens found in the human gut, such as *Methanobrevibacter smithii* and *Methanosphaera stadtmanae*, and thermophilic methanogens, such as *Methanocaldococcus villosus* and *Methanothermobacter thermautotrophicus* (6–8). However, genes and proteins important for growth on surfaces have largely remained uncharacterized in these organisms. *Methanococcus maripaludis* strain S2 was shown to attach to surfaces in a pilus- and archaellum-dependent manner (9), but the roles of these structures in surface-associated growth remain underexplored. While *M. maripaludis* strain S2 was not found to readily form a monoculture biofilm, it can associate with a syntrophic bacterial partner (10). Additionally, some strains of *M. maripaludis* have been found to associate with Fe^0, form biofilms, and corrode the metal surface (11).

Both O-linked and N-linked glycosylation are found in archaea, but the enzymes responsible for O-linked glycosylation are uncharacterized (12). Archaeal N-linked glycosylation of surface structures (pili, archaella, and S-layers) is catalyzed by the oligosaccharyltransferase AglB and occurs on the asparagine of the conserved N-X-S/T motif (where X is any amino acid other than proline) (12, 13). In *M. maripaludis* strain S2, both archaella and pili contain N-glycosylations (14–17). The S-layer of *M. maripaludis* strain S2 is not known to contain N-glycosylations, but other members of the genus, such as *Methanococcus voltae*, possess an S-layer glycoprotein (18). Glycosylation of pili, archaella, and S-layers can be important for maintaining the stability of these proteins when cells are growing in extreme environments (e.g., high temperature, high salinity, or low pH) (4, 19, 20). For example, in *Haloferax volcanii*, deletion of *aglB* resulted in unstable S-layer architecture, defective pilus-dependent surface attachment, aberrant biofilm formation, decreased efficiency of the fusion-based mating system, and defects in archaellum-mediated motility (4, 21–24).

In an effort to better understand the genetic underpinnings of surface-associated growth in a member of the methanogenic archaea, we undertook a comparative study of *M. maripaludis* strains S2 and JJ. We found that only strain JJ is capable of robust colonization of glass and metal surfaces and this is likely dependent on AglB-dependent glycosylation of the S-layer. The S-layer of *M. maripaludis* strain S2 is not glycosylated, and this strain did not grow attached to any surfaces tested. Interestingly, surface-attached growth was not dependent on pili or archaella in medium with H_2 as an electron donor, suggesting that S-layer glycosylation can overcome defects in pilus- and archaellum-dependent surface attachment. We also found that surface-associated growth can enhance rates of anaerobic Fe^0 oxidation in strains engineered to oxidize the metal surface. These data provide initial insights into the genetic and molecular underpinnings of surface-associated growth in *M. maripaludis* and suggest that S-layer glycosylation is important for surface-dependent processes.

RESULTS

***M. maripaludis* strain JJ grows as a surface-attached community in static cultures.** When *M. maripaludis* stain JJ is grown in static liquid cultures with either H_2 or formate as the electron donor for growth, surface-attached biomass accumulates on the side of culture tubes (Fig. 1). This visible biomass could be stained with crystal violet, and retained stain could be solubilized and quantified by absorbance at 590 nm (25). Visible attached biomass was absent in cultures grown with agitation. In cultures grown with H_2 as the sole electron donor for methanogenesis, surface growth occurred at the atmosphere-liquid interface; this growth pattern is reminiscent of growth of bacterial biofilms at the air-liquid interface of standing cultures under oxic conditions (25, 26). In aerobic bacteria, this pattern is due to oxidant-starved populations growing preferentially at the air-liquid interface to gain access to oxygen from the atmosphere. In the case of *M. maripaludis* strain JJ, we hypothesize that growth at the atmosphere-liquid interface of standing cultures was due to reductant-starved populations (i.e., H_2-starved cells) growing preferentially at the atmosphere-liquid interface to gain access to H_2 from the atmosphere. Consistent with this,

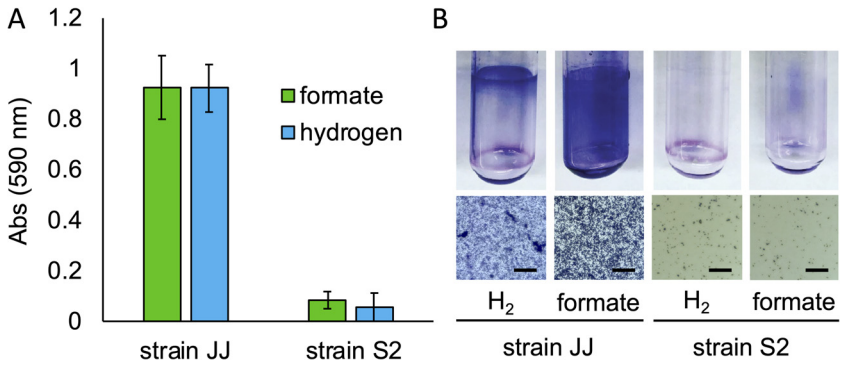

FIG 1 Surface attached growth of *M. maripaludis* strains. (A) Quantification of surface-associated biomass stained with crystal violet from wild-type *M. maripaludis* strains JJ and S2 grown in medium with either H_2 or formate as the electron donor. Data are averages and standard deviations for three cultures. (B) Images of stained Balch tubes from strains JJ and S2 (top) and cells attached to microscope coverslips. Bar = 25 μm.

when cultures were grown with the soluble electron donor formate, surface-attached biomass was readily apparent throughout the culture tube (Fig. 1). Surface-attached growth was not observed in either condition with *M. maripaludis* strain S2.

The oligosaccharyltransferase AglB is essential for surface-associated growth. We hypothesized that differences in surface-associated growth between *M. maripaludis* strains JJ and S2 were due to differences in the abundance or structure of cell surface appendages. Pili and archaella are necessary for surface attachment in *M. maripaludis* strain S2, and both of these structures are composed of glycoproteins (12, 15–17, 27, 28). *M. maripaludis* mutants that are defective for N-glycosylation of archaella and pili are nonmotile (29), and defects in pilus N-glycosylation result in aberrant biofilm formation in other archaea (4). The genomes of strains S2 and JJ are 95% identical (2-way average nucleotide identity) (30–33), but there are likely differences in how these strains glycosylate surface appendages. For example, strain JJ lacks at least one N-X-S/T site on the major pilin, EpdE, which is a verified glycosylation site in strain S2 (15, 34). Glycosylation differences may affect how these proteins bind extracellular substrates and surfaces.

Because disruption of *aglB* resulted in aberrant biofilm formation in other archaea (4), we generated a mutant that lacks *aglB* (the Δ*aglB* strain) in strain JJ. We additionally analyzed mutants that lacked either pili (the Δ*epdJKL* strain) or archaella (the Δ*flaK* strain) (34) and generated a double mutant strain that lacked both (the Δ*epdJKL* Δ*flaK* strain). Cultures were analyzed by crystal violet staining over the course of 96 h, with H_2 provided as the electron donor to allow sufficient time for cultures to reach stationary phase. The extended incubation period necessary for static cultures to reach stationary phase is likely a result of poor diffusion of H_2 into the aqueous phase. There was not a significant difference in the density of surface growth between the wild type, the Δ*epdJKL* strain, the Δ*flaK* strain, and the Δ*epdJKL* Δ*flaK* strain, as determined by amount of crystal violet stain taken up by attached biomass, and the Δ*aglB* strain was defective for surface-associated growth (Fig. 2A). No growth defects were observed in planktonic culture for mutant strains lacking *aglB*, *flaK*, or *epdJKL* (see Fig. S1 in the supplemental material).

To verify that surface attached material was composed of cellular biomass, we grew cultures on glass coverslips. This allowed visualization of the crystal violet-stained surface-associated community under a microscope (Fig. 2B). Biomass was composed of both individually attached cells and microcolonies up to ~50 μm in diameter. Attached cells were present in all cultures, with the fewest seen in the Δ*aglB* strain, suggesting that the crystal violet quantification was correlated with growth. Interestingly, microcolonies were present in wild-type cultures but absent from the Δ*flaK* strain, suggesting a role for archaella in microcolony formation.

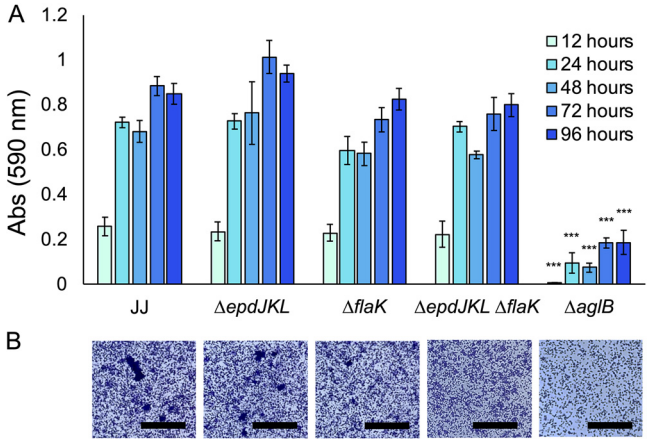

FIG 2 Growth of *M. maripaludis* strain JJ and mutants in standing culture with H_2 as the electron donor. (A) Quantification of surface-associated biomass from cultures grown in McCas medium with H_2 provided as the sole electron donor and stained with crystal violet. Cultures were grown without agitation for 96 h, the amount of time needed to reach stationary phase. Data are averages and standard deviations from four independent experiments. (B) Surface-attached biomass from microscope coverslips submerged in McCas medium with H_2 provided as the sole electron donor. Images were taken from the center of the coverslip near the area corresponding to the atmosphere-liquid interface. Bar = 50 μm. ***, $P < 0.001$.

Archaella play a role in surface-associated growth when formate is the sole electron donor for methanogenesis. To test the role of pili, archaella, and AglB in surface-associated growth with formate as the sole electron donor, we analyzed growth using the crystal violet assay and cultures grown with formate. Cultures were analyzed by crystal violet staining over the course of 24 h to reflect the amount of time it takes static cultures of *M. maripaludis* to reach stationary phase in formate medium (Fig. 3). Surface colonization was lower in both the Δ*flaK* strain and the Δ*epdJKL* Δ*flaK* strain, suggesting a role for archaella in surface colonization. The Δ*epdJKL* strain was indistinguishable from the wild type at most time points analyzed, suggesting that pili are not essential for surface growth. Because archaella are known to be important for attachment to glass (9), we hypothesize that decreased surface colonization is due to an

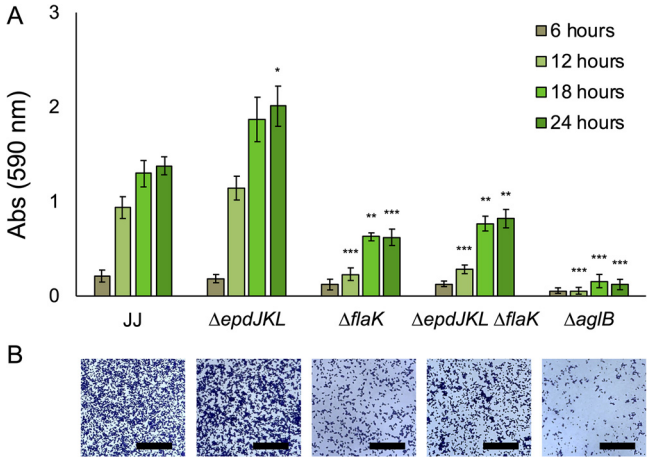

FIG 3 Growth of *M. maripaludis* strain JJ and mutants in standing culture with formate as the electron donor. (A) Quantification of surface-associated biomass from cultures grown in McCas-formate medium and stained with crystal violet. Cultures were grown without agitation for 24 h, the amount of time needed to reach stationary phase. Data are averages and standard deviations from four independent experiments. (B) Surface-attached biomass from microscope coverslips submerged in McCas-formate medium. Images were taken from the center of the coverslip. Bar = 50 μm. *, $P < 0.05$; **, $P < 0.01$; ***, $P < 0.001$.

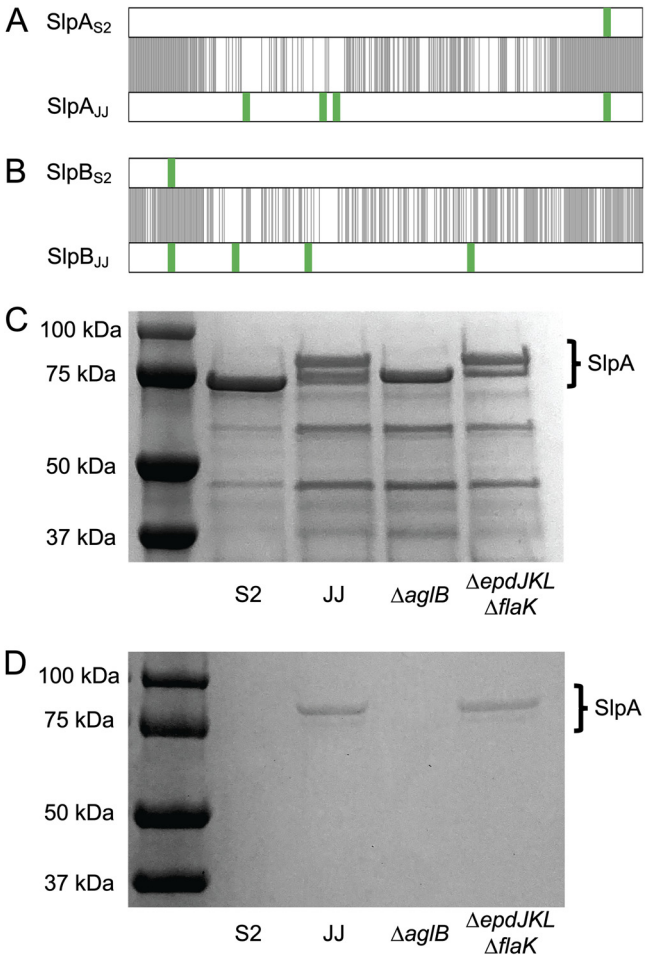

FIG 4 Glycosylation of the S-layer protein of *M. maripaludis* strain JJ. Alignment of S-layer proteins SlpA (A) and SlpB (B). Black lines indicate positions of amino acid identity and putative N-linked glycosylation sites (N-X-S/T, where X is any amino acid other than proline) are indicated in green. (C) Coomassie stained SDS-PAGE gel of the supernatant from whole cells that were suspended in protoplasting buffer. SlpA proteins were identified by mass spectrometry. (D) Periodic acid-Schiff stained SDS-PAGE gel showing the presence of glycoproteins.

attachment defect, but more experimentation is necessary to verify this. Similar to what was seen in H_2-grown static cultures, the Δ*aglB* strain was defective for surface-associated growth, and attached cells were observed microscopically in all mutants, with the fewest being seen in the Δ*aglB* strain.

The S-layer of *M. maripaludis* strain JJ is a glycoprotein. The fact that the Δ*epdJKL* Δ*flaK* strain displayed surface growth similar to that of the wild type in medium with H_2 suggested that the phenotype observed in the Δ*aglB* strain was due to a defect in glycosylation of another cell surface structure. In addition to pili and archaella, AglB is capable of glycosylating the S-layer protein; therefore, we hypothesized that differences in S-layer glycosylation are responsible for surface colonization in strain JJ and a lack of surface-associated growth in strain S2. To determine whether there are differences in S-layer glycosylation, we compared the primary sequence of the surface layer proteins (Slp) of both strains. *M. maripaludis* has two surface layer proteins, SlpA and SlpB. Between the two strains, SlpA exhibits ~63% amino acid identity and SlpB has ~60% amino acid identity. These proteins are most similar at the N and C termini. Both SlpA and SlpB from strain JJ contain 4 putative N-linked glycosylation sites (N-X-S/T motif); each protein from strain S2 contains a single putative N-linked glycosylation site (Fig. 4A and B).

Due to the presence of several putative N-linked glycosylation sites in the S-layer proteins of strain JJ that are absent in strain S2, we hypothesized that these proteins are differentially glycosylated. To test this, we purified S-layer proteins from each strain. Protoplasts of strain S2, strain JJ, the Δ*aglB* strain, and the Δ*epdJKL* Δ*flaK* strain were isolated by washing and suspending cells in protoplasting buffer (35, 36) and separating the soluble S-layer protein from protoplasts by centrifugation. After separation of the supernatant fraction by sodium dodecyl sulfate-polyacrylamide gel electrophoresis (SDS-PAGE) and staining with Coomassie blue, S-layer proteins from both strain S2 and the Δ*aglB* strain resolved as a single band and S-layer proteins from strain JJ and the Δ*epdJKL* Δ*flaK* strain separated as two distinct bands (Fig. 4C). Protein bands isolated from strain S2, strain JJ, and the Δ*aglB* strain were further analyzed by tandem mass spectrometry at the University of Minnesota Center for Mass Spectrometry and Proteomics and verified as SlpA, the major constituent of the *M. maripaludis* S-layer. SlpB was not identified in any samples analyzed. The additional SlpA band of apparently higher molecular mass in strain JJ that was missing in the Δ*aglB* strain suggests that the two bands observed in wild-type JJ are alternative glycosylation states of SlpA. Lower-molecular-mass bands are also present on these gels, presumably resulting from cell lysis during the protoplasting procedure.

To further verify the presence of differentially glycosylated SlpA protein in strain JJ, we performed a periodic acid-Schiff (PAS) stain (37, 38). The PAS reagent specifically stains glycoproteins and reacted only with proteins from strain JJ and the Δ*epdJKL* Δ*flaK* strain (Fig. 4D). There was no apparent staining in strain S2 or the Δ*aglB* strain. Taken together, these data suggest that differential S-layer N-linked glycosylation is responsible for increased surface-associated growth in strain JJ. Attempts to mutagenize *slp* by allelic replacement, by expressing *slpA* or *slpB* from strain S2 in strain JJ (or vice versa), or by alanine or glutamine substitution of the asparagine residues of the N-linked glycosylation motif (either single replacements or in combination) were unsuccessful. In all cases, assuming equal fitness of the wild-type and mutant alleles, mutagenesis by allelic replacement should have resulted in 50% recovery of the mutant allele among screened colonies (36); however, only the wild-type allele was recovered in each case. We also attempted expression of *slp* genes in *trans* on a replicative vector without success. We hypothesize that an inability to perturb S-layer proteins is due to a requirement for functional Slp to maintain S-layer integrity.

Surface appendages and AglB-dependent glycosylation are important for growth on metals. In addition to glass surfaces, *M. maripaludis* attaches to metals (9), and in some strains, metal-associated biofilms are thought to drive oxidation and corrosion of the metal surface (11, 39). To test the role of AglB-dependent glycosylation in growth on a metal surface, cultures were incubated in medium with solder tabs composed of 99.6% nickel, and surface-attached biomass was quantified using crystal violet. Growth patterns were similar to what was observed on glass. The Δ*aglB* strain was defective for surface-associated growth with either H_2 or formate as the electron donor, and the Δ*flaK* and Δ*epdJKL* Δ*flaK* strains displayed an ~50% reduction in surface observed biomass when formate was provided as the sole electron donor (Fig. 5).

AglB-dependent glycosylation enhances iron corrosion in strains capable of Fe^0 oxidation. Several strains of *M. maripaludis* have been identified that are capable of oxidizing Fe^0 to Fe^{2+} (11, 39, 40). This activity is dependent on a hydrogenase that is thought to be secreted outside the cell through a twin-arginine transporter (Tat) (39). The genes encoding these proteins are absent from strain JJ; however, we sought to determine whether surface-associated growth would enhance Fe^0 oxidation. A genomic region encoding the putative Tat transporter and secreted hydrogenase from *M. maripaludis* strain OS7 was synthesized, placed on the replicative vector pLW40neo to generate pLW40-iron (Fig. 6A), and introduced into strain JJ, the Δ*aglB* strain, and the Δ*epdJKL* Δ*flaK* strain. Using reverse transcriptase PCR, we verified that these genes are heterologously expressed (Fig. S2). Cultures of each strain were incubated in medium with Fe^0 (as a wire nail inserted into the culture tube), and Fe^{2+} production was monitored. All three strains accumulated Fe^{2+} in the culture supernatant, consistent with heterologous expression and extracellular activity of the iron-corroding hydrogenase (Fig. 6B). Furthermore,

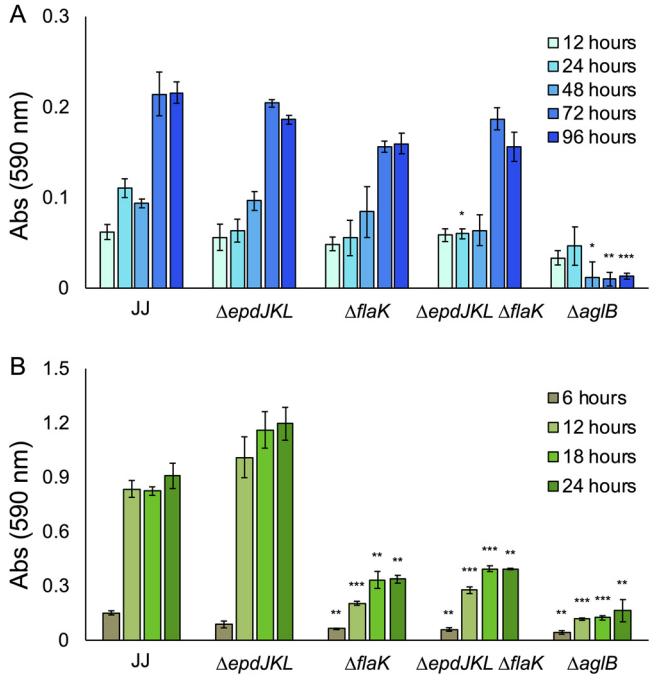

FIG 5 Growth of *M. maripaludis* strain JJ and mutants attached to 99.6% nickel solder tabs. (A and B) Quantification of surface-associated biomass stained with crystal violet from cultures grown in McCas medium with H_2 provided as the sole electron donor (A) or McCas-formate (B). Cultures were grown without agitation. Data are averages and standard deviations from three independent experiments. *, $P < 0.05$; **, $P < 0.01$; ***, $P < 0.001$.

control experiments demonstrated that a strain lacking genes for the hydrogenase but harboring genes for the Tat secretion system were unable to oxidize Fe^0 (Fig. S3).

For strains carrying pLW40-iron, rates of Fe^0 oxidation were significantly higher in strain JJ and the Δ*epdJKL* Δ*flaK* strain than the Δ*aglB* strain. Fe^{2+} did not accumulate in a culture of strain JJ lacking the pLW40-iron plasmid. We additionally incubated cultures in formate medium with Fe^0 to determine whether a condition where strain JJ is known to associate with surfaces impacts Fe^0 oxidation rates. Formate medium was used to allow high levels of surface attachment (Fig. 1), and, under this condition, formate is present as an electron donor for CO_2 reduction. In the presence of both formate and Fe^0, rates of Fe^0 oxidation were significantly higher in strain JJ and the Δ*epdJKL* Δ*flaK* strain than the Δ*aglB* strain (Fig. 6C). We were unable to quantify surface-associated biomass via crystal violet staining due to high background staining of the Fe^0 surface, but all four cultures grew to similar optical density at 600 nm (OD_{600}) in the presence of both formate and Fe^0, suggesting that different Fe^0 oxidation rates were not due to differences in total biomass.

DISCUSSION

Organisms from across the tree of life grow as biofilms; however, the molecular basis of surface-associated growth is poorly studied in methanogens. Studies on surface attachment in *M. maripaludis* have primarily focused on the role of pili and archaella (9). However, these experiments were performed in strain S2, a strain that, as we have shown here, is incapable of robust surface colonization. While strain S2 has been shown to form pellicles, a layer that forms at the atmosphere-liquid interface of standing cultures, and coculture biofilms with *Desulfovibrio vulgaris* (10, 41), to our knowledge, our work is the first molecular characterization of surface grown axenic cultures of *M. maripaludis* and the first identification of the S-layer glycoprotein supporting surface-associated growth in a methanogen.

In addition to *M. maripaludis*, several other methanogens have been reported to grow attached to surfaces. *M. villosus* forms a surface-attached community in laboratory

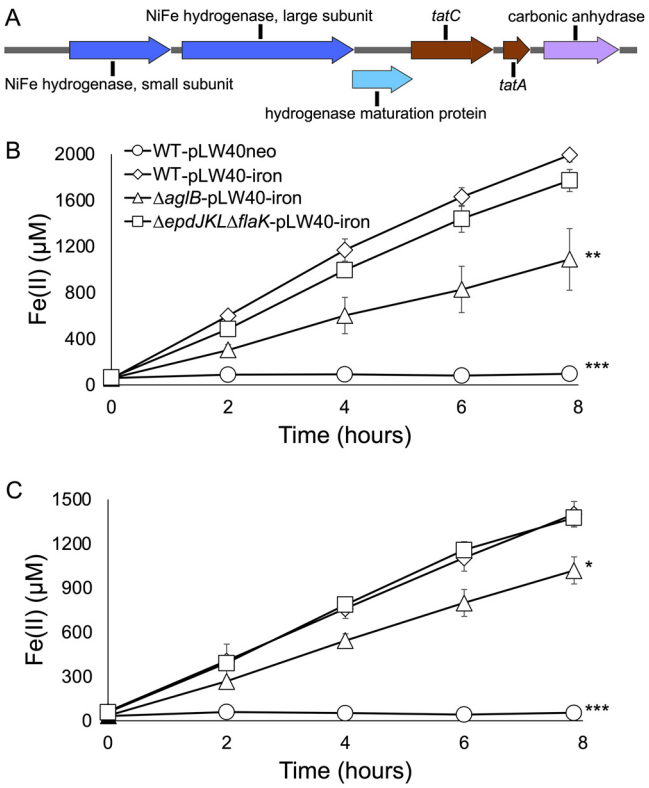

FIG 6 Fe^0 oxidation by *M. maripaludis* strain JJ containing a putative genomic island for Fe^0 corrosion. (A) Map of genes for Fe^0 corrosion from *M. maripaludis* strain OS7. The mapped region, corresponding to nucleotides 1,131,633 to 1,137,117 from strain OS7, was introduced into *M. maripaludis* strain JJ or the indicated mutant strains on pLW40neo (pLW40-iron). The map was generated using SnapGene software (Insightful Science). (B and C) Fe^{2+} production in the presence of Fe^0 in the absence (B) or presence (C) of formate. Fe^{2+} production was not observed in the absence of genes from panel A. Rates of Fe^{2+} production were compared to that of wild-type strain JJ containing pLW40-iron. Data are averages and standard deviations from three independent experiments. *, $P < 0.05$; **, $P < 0.01$; ***, $P < 0.001$.

culture (7), and the S-layer protein of this organism contains several N-X-S/T motifs, suggesting that it may be a glycoprotein (42). Biofilms have also been observed in members of the order *Methanosarcinales*, *M. thermautotrophicus*, and human gut-associated methanogens such as *M. smithii* (6, 8). Cell surface structures vary among these groups, with some possessing S-layer glycoproteins and others possessing cell walls composed of pseudomurein (43); it remains to be determined whether glycans within the pseudomurein layer also support growth on surfaces.

AglB glycosylates both pili and archaella in *M. maripaludis* (12, 15, 17). We did not observe a defect in surface-associated biomass for the Δ*epdJKL* mutant at any of the time points assayed. Although the Δ*flaK* mutant displayed surface attached growth when cultures were grown on formate, biomass was reduced compared to that of the wild type. The Δ*epdJKL* Δ*flaK* double mutant was phenotypically similar to the Δ*flaK* mutant. These data suggest that archaella may be important in formate media (Fig. 3). The lack of a clear phenotypic difference between the wild type and the Δ*epdJKL* mutant in our assays raises the possibility that pili are not involved in surface-attached growth. They may have a different function; for example, we recently found that strain JJ is naturally competent and that pili are essential for DNA uptake (34).

It was recently demonstrated that *M. maripaludis* is capable of chemotaxis toward hydrogen (41). Our observation that a Δ*flaK* mutant strain grows at the atmosphere-liquid interface of standing cultures with H_2 as the electron donor suggests that, under laboratory growth conditions, chemotaxis is not essential for surface-associated growth. Syntrophic growth of biofilm aggregates is increased under conditions where efficient H_2

TABLE 1 *M. maripaludis* strains used in this study

Strain	Reference
S2 Δ*upt*	52
JJ Δ*upt*	53
JJ Δ*upt* Δ*epdJKL*	34
JJ Δ*upt* Δ*flaK*	34
JJ Δ*upt* Δ*epdJKL* Δ*flaK*	This study
JJ Δ*upt* Δ*aglB*	This study

transfer is required (44), and growth on metals is enhanced when surface-attached cells secrete a hydrogenase through a twin-arginine transporter to enhance H_2 transfer (39). Therefore, we hypothesize that surface-attached growth is advantageous for cells growing near a nutrient source. Our finding that Fe^0 corrosion rates are 50% to 100% higher in *aglB*$^+$ strains (Fig. 6) supports this hypothesis; therefore, we hypothesize that strains carrying the native genomic island for Fe^0 oxidation rely on AglB-dependent glycosylation to robustly colonize the metal surface (39, 40). These observations suggest that growth at the surface or in association with other cells is H_2 dependent, ensures that cells have access to H_2, and may limit diffusive loss of H_2 to the environment.

M. maripaludis attaches efficiently to a variety of surfaces, such as glass, metals, silicon, or other cells (9). Our data suggest that surface growth and, in the case of strains containing genes for a putative extracellular hydrogenase, Fe^0 oxidation are enhanced by AglB-dependent glycosylation of the S-layer protein. While AglB is additionally responsible for glycosylation of pili and archaella, the fact that the Δ*epdJKL* Δ*flaK* mutant strain was capable of surface-attached growth under several experimental conditions suggests that the phenotype of the Δ*aglB* mutant strain was not a result of a glycosylation defect in cell surface appendages. While further work is necessary to determine if S-layer glycoproteins or cell wall glycosylation enhance surface-associated growth in other methanogens, our results provide initial insights into the role of glycoproteins in methanogenic biofilms.

MATERIALS AND METHODS

Strains, medium, and planktonic growth conditions. Strains used in this study are listed in Table 1. For both *M. maripaludis* strains JJ and S2, the wild-type strain used in all experiments is a mutant lacking the gene encoding uracil phosphoribosyltransferase (*upt*) (34, 45). Mutants lacking archaella and pili are described in reference 34. A mutant lacking both archaella and pili was constructed using the plasmids from reference 34. A mutant lacking *aglB* was constructed as described in "Molecular techniques" below. All strains were grown in McCas medium or McCas-formate medium (45) at 37°C with agitation, except that Na_2S was replaced with $(NH_4)_2S$ (34) for liquid medium. For growth with H_2 as the electron donor, tubes were pressurized to 280 kPa with an 80% H_2–20% CO_2 gas mix. For growth with formate as the electron donor, tubes were pressurized to 280 kPa with an 80% N_2–20% CO_2 gas mix. All cultures used in biofilm growth experiments were preadapted to the appropriate medium before use in experiments. When necessary, neomycin (1 mg ml^{-1}) or 6-azauracil (0.25 mg ml^{-1}) was added to medium. *Escherichia coli* was grown at 37°C in lysogeny broth or on lysogeny broth agar plates supplemented with ampicillin (50 μg ml^{-1}).

Growth on glass. Surface-attached biomass was stained and quantified using a modification of the crystal violet method that works for both bacteria and archaea (25, 26, 46, 47). *M. maripaludis* strains were grown as surface-attached communities in standing Balch tubes containing 5 ml of growth medium. Cultures were preadapted to growth with H_2 or formate as the electron donor in overnight shaking cultures to stationary phase (OD_{600} of 1.0 to 1.2 for H_2 medium and 0.5 to 0.6 for formate medium). Fresh medium was inoculated 1/25 or 1/50 (vol/vol) and left standing (no agitation) at 37°C for the amount of time indicated in each figure. After growth, tubes were pressurized to 138 kPa and inverted three times by hand to remove loosely attached biomass. Residual medium was removed by inverting the tube, inserting a 23-gauge needle, and allowing pressure to drive medium out of the tube. Balch tubes were opened under an oxic atmosphere, filled with 5 ml of 0.1% crystal violet, and stained for 10 min. Residual stain was removed by washing the tubes 3 times with water, and tubes were air dried. To destain and quantify attached biomass, 5 ml of 30% acetic acid was added to each tube and tubes were vortexed at maximum speed for 5 s. Two hundred microliters of the 30% acetic acid solution containing crystal violet was transferred to a 96-well plate, and absorbance was measured at 590 nm using a SpectraMax M2e microplate reader (Molecular Devices). Experiments were performed in quadruplicate and normalized to a control tube without cell material.

Growth on nickel. To grow biomass attached to nickel surfaces, 0.15- by 8- by 100-mm solder tabs composed of 99.6% nickel (U.S. Solid; number JFPNS00006) were used. Stationary-phase cultures were inoculated 1/25 (vol/vol) into 10 ml of the appropriate medium inside a 15-ml Falcon conical tube containing one solder tab. These were placed in a test tube rack and packaged into a stainless steel anaerobic

incubation vessel with moistened paper towels lining the bottom and a reservoir containing 15 ml 25% $Na_2S \cdot 9H_2O$. For growth with H_2 as the electron donor, the headspace of the vessel was exchanged to an H_2-CO_2 gas mix (80:20), and for growth with formate as the electron donor, the headspace was N_2-CO_2 (80:20), both at 140 kPa. The anaerobic incubation vessels were incubated at 37°C for the amount of time indicated in each figure. After growth, vessels were opened under an oxic atmosphere and solder tabs were cleaned by blotting on a paper tower and transferred to a 12- by 75-mm glass tube containing 5 ml of 0.1% crystal violet for 10 min. Solder tabs were washed 3 times in water and transferred to a new 12- by 75-mm glass tube containing 5 ml of 30% acetic acid to destain. Two hundred microliters of the 30% acetic acid solution containing crystal violet was transferred to a 96-well plate, and absorbance was measured at 590 nm. Experiments were performed in triplicate and normalized to a control tube without cell material.

Growth in the presence of Fe^0. Galvanized 6-cm, 140-g wire iron nails were used as a source of Fe^0 in culture medium. Metal was treated to remove the galvanic coating by soaking in 3 N HCl for 5 min before neutralizing the acid in a sodium bicarbonate solution. Metal was immediately moved into a Coy anaerobic chamber (2 to 3% H_2, 10% CO_2, balance N_2 in the atmosphere) to prevent oxidation. A sterilized magnetic rod was used to move treated Fe^0 into and out of Balch tubes containing 5 ml of either McCas or McCas-formate medium (both under an N_2-CO_2 atmosphere). The experiment was started by inoculation with 0.5 ml of an overnight culture ($OD_{600} \sim 1.2$) of the appropriate strain or 0.5 ml of sterile medium that was prereduced with $(NH_4)_2S$. No additional sulfide was added. The sterile medium was included as a control to account for Fe^{2+} present in McCas or McCas-formate. Cultures were incubated at 37°C without agitation. All experiments were performed in triplicate.

To measure Fe^{2+} accumulation, 0.1 ml of culture material was removed under anoxic conditions at the time points indicated in Fig. 6 and immediately mixed with 0.1 ml of 1 N HCl. Under these conditions, Fe^{2+} is stable in the presence of atmospheric O_2. Fe^{2+} was measured following the protocol in references 48 and 49. Briefly, 50 μl of the culture-HCl mixture was mixed with 300 μl of ferrozine assay reagent {2 g liter^{-1} ferrozine [3-(2-pyridyl)-5,6-diphenyl-1,2,4-triazine-*p*,*p*′-disulfonic acid], 23.8 g liter^{-1} HEPES [pH 7]}, and absorbance was quantified at 625 nm. Samples were normalized to the sterile medium control and compared to standards of $FeSO_4$ in 0.5 N HCl.

Microscopic analysis of surface growth. Cultures of each strain were grown overnight to stationary phase in McCas medium and moved into a room-temperature Coy anaerobic chamber (2 to 3% H_2, 10% CO_2, balance N_2 in the atmosphere). Sterile McCas or McCas-formate medium was inoculated 1/25 with the overnight culture, and 2 ml was aliquoted into individual wells of a tissue culture-treated 12-well polystyrene plate (Falcon; number 353043). A 22- by 22-mm number 1.5 glass coverslip was added to each well (Globe Scientific Inc.; number 1404-15). The plates were transferred to a 7-liter stainless-steel anaerobic incubation vessel with moistened paper towels lining the bottom and a reservoir containing 15 ml 25% $Na_2S \cdot 9H_2O$. For growth with H_2 as the electron donor, the headspace of the vessel was exchanged to an H_2-CO_2 gas mix (80:20), and for growth with formate as the electron donor, the headspace was N_2-CO_2 (80:20), both at 140 kPa. The anaerobic incubation vessels were moved to a 37°C incubator and left for 24 h. After incubation, vessels were moved into the anaerobic chamber and degassed under a stream of N_2-CO_2 for 20 min before opening. Coverslips with attached biomass were washed by dipping in a *Methanococcus* salts buffer (22 g liter^{-1} NaCl, 5 g liter^{-1} $NaHCO_3$, 0.34 g liter^{-1} KCl, 2.8 g liter^{-1} $MgCl_2 \cdot 6H_2O$, 3.5 g liter^{-1} $MgSO_4 \cdot 7H_2O$, 0.14 g liter^{-1} $CaCl_2 \cdot 2H_2O$) and placed into a well of a new 12-well plate, with each well containing 4 ml of 2% glutaraldehyde in *Methanococcus* salts buffer. Biomass was fixed in this solution for 20 min. After fixation, the plate was moved out of the anaerobic chamber, and coverslips were transferred to a new 12-well plate, with each well containing 4 ml of 0.1% crystal violet. Biomass was stained for 10 min, and excess dye was washed off by dipping the coverslip in water 5 times. The coverslip was left to air dry before imaging. Microscopic analysis was performed on an ECHO Revolve R4 hybrid microscope in the upright orientation with an extralong-working-distance (ELWD) universal condenser (numerical aperture [NA], 0.30; working distance [WD], 73 mm). Images were taken with either a 20× fluorite (ELWD; NA, 6.6 to 7.8 mm) or 40× fluorite (NA, 0.75 and 0.51 mm) lens objective. Images were collected from the middle of the slide near the location of the atmosphere-liquid interface.

Molecular techniques. To generate a mutant lacking *aglB*, genomic regions flanking the gene were PCR amplified with primers JJ_AglB_USF (5′-CCATCACACTGGCGGCCGCAAGACCGTTGAAACCTGCAAG) and JJ_AglB_USR (5′-TTATAAAAATTCACCCATAATCCTCCTCCAAAATTTTTATC) to amplify an ~500-bp region upstream of *aglB* and JJ_AglB_DSF (5′-ATGGGTGAATTTTTATAATTTTGAGATTTAATTTTTTTACC) and JJ_AglB_DSR (5′-GGCGAATTGGGCCCTCTAGATGAAAGGTTGTAGTCTGCAAG) to amplify an ~500-bp region downstream of *aglB*. The resulting PCR products were combined with XbaI- and NotI-digested pCRUptNeo and assembled by Gibson Assembly (50). All enzymes were purchased from New England Biolabs. The assembled vector was electroporated into *E. coli* DH5α. The resulting plasmid, pCRUptNeo-Δ*aglB*, was purified using a PureLink quick plasmid miniprep kit (Invitrogen). To transform *M. maripaludis* strain JJ, pCRUptNeo-Δ*aglB* was introduced as described elsewhere (34). After transformation, culture was transferred to McCas medium containing neomycin and allowed to grow for 2 days. This selected for a population of merodiploids containing both wild-type and mutant alleles. One drop was transferred to medium without selection and grown overnight to allow the merodiploid to resolve in a subset of the population, and cultures were plated on solid medium containing 6-azauracil for counterselection. Colonies were allowed to grow for 3 days before screening by PCR to identify mutants. Mutants were streak purified before use, and the sequence of the mutant allele was verified with Sanger sequencing (University of Minnesota Genomics Center).

To generate *M. maripaludis* strains capable of Fe^0 oxidation, a genomic region from *M. maripaludis* strain OS7 encoding a putative twin arginine transporter and a putative secreted hydrogenase was

synthesized by Bio Basic, Inc., and placed into XhoI- and SpeI-cut pLW40neo (51). The genomic region corresponded to base pairs 1,131,633 to 1,137,117 of the *M. maripaludis* strain OS7 genome (NCBI accession number GCA_000828555.1). The resulting plasmid was introduced into *M. maripaludis* strain JJ or the appropriate mutant strains via the polyethylene glycol (PEG) method of transformation (35).

S-layer purification and analysis. To purify the S-layer glycoprotein, strains were grown overnight in McCas medium to a final OD_{600} of 0.8 to 1.0. Tubes were opened under an oxic atmosphere, and 4.5 ml of culture material was collected by centrifugation in 1.7-ml microcentrifuge tubes (3 spins at 13,000 $\times$ *g* for 1 min). Residual supernatant was removed, and the cell pellet was suspended in 0.6 ml of protoplasting buffer (0.35 M sucrose, 0.38 M NaCl, 50 mM Tris [pH 7.5]) by gentle pipetting (35). Cells were pelleted by centrifugation (13,000 $\times$ *g* for 1 min), and the supernatant was concentrated to $\sim$50 μl using a Vivaspin 500 column (3-kDa molecular weight cutoff) protein concentrator following the manufacturer's instructions. The concentrated supernatant was subjected to sodium dodecyl sulfate polyacrylamide gel electrophoresis (SDS-PAGE) using a 4 to 20% Criterion TGX precast midi-protein gel (Bio-Rad) followed by staining with Coomassie brilliant blue R-250. A second gel was used to cut out bands from proteins purified from wild-type strain S2, wild-type strain JJ, and the JJ Δ*aglB* mutant. These cut bands were submitted to the University of Minnesota Center for Mass Spectrometry and Proteomics. All four purified bands were identified as S-layer protein A (SlpA).

To specifically stain glycoproteins, purified S-layer preparations were separated by SDS-PAGE and subjected to periodic acid-Schiff staining using a microwave-assisted protocol as described elsewhere (38). Briefly, gels were fixed by heating for 1 min in 50 ml of 50% MeOH in a 700-W microwave oven (Farberware) and washed in H_2O. The gel was oxidized by heating for 45 s in a solution of 1% periodic acid and then washed by heating for 1 min in H_2O three times. The gel was flooded with 25 ml Schiff's reagent (Fisher Chemical) and heated for 30 s, followed by a wash with 5% sodium metabisulfite (heated for 1 min). Finally, the gel was washed at room temperature with 0.1% sodium metabisulfite followed by several washes in H_2O. The sodium metabisulfite is necessary to reduce background staining. Glycoproteins stained as pink/purple bands.

Statistical analysis. Data sets derived from experiments with mutant strains were compared to those for the wild type. Data are presented as means and standard deviations. One-way analysis of variance (ANOVA) was used to compare the means of groups. This was followed by *post hoc t* tests between the wild-type and mutant strains with corrections based on Dunn's multiple-comparison test. Differences were considered significant if adjusted *P* values were <0.05.

Data availability. Mass spectrometry data from the S-layer analyses are freely available at the Data Repository for the University of Minnesota (DRUM): https://doi.org/10.13020/fhxh-n267.

SUPPLEMENTAL MATERIAL

Supplemental material is available online only.

SUPPLEMENTAL FILE 1, PDF file, 0.2 MB.

ACKNOWLEDGMENTS

We thank Madison Loppnow for assistance in the laboratory.

This work was sponsored by a Young Investigator Program award to K.C.C. from the Army Research Office, grant number W911NF-19-1-0024. D.R.F. was supported by the National Science Foundation Graduate Research Fellowship Program under grant number CON-75851.

REFERENCES

1. Flemming H-C, Wuertz S. 2019. Bacteria and archaea on Earth and their abundance in biofilms. Nat Rev Microbiol 17:247–260. https://doi.org/10.1038/s41579-019-0158-9.
2. van Wolferen M, Orell A, Albers S-V. 2018. Archaeal biofilm formation. Nat Rev Microbiol 16:699–713. https://doi.org/10.1038/s41579-018-0058-4.
3. Orell A, Fröls S, Albers S-V. 2013. Archaeal biofilms: the great unexplored. Annu Rev Microbiol 67:337–354. https://doi.org/10.1146/annurev-micro-092412-155616.
4. Esquivel RN, Schulze S, Xu R, Hippler M, Pohlschroder M. 2016. Identification of *Haloferax volcanii* pilin N-glycans with diverse roles in pilus biosynthesis, adhesion, and microcolony formation. J Biol Chem 291:10602–10614. https://doi.org/10.1074/jbc.M115.693556.
5. Zolghadr B, Klingl A, Koerdt A, Driessen AJM, Rachel R, Albers S-V. 2010. Appendage-mediated surface adherence of *Sulfolobus solfataricus*. J Bacteriol 192:104–110. https://doi.org/10.1128/JB.01061-09.
6. Bang C, Ehlers C, Orell A, Prasse D, Spinner M, Gorb SN, Albers S-V, Schmitz RA. 2014. Biofilm formation of mucosa-associated methanoarchaeal strains. Front Microbiol 5:353. https://doi.org/10.3389/fmicb.2014.00353.
7. Bellack A, Huber H, Rachel R, Wanner G, Wirth R. 2011. *Methanocaldococcus villosus* sp. nov., a heavily flagellated archaeon that adheres to surfaces and forms cell-cell contacts. Int J Syst Evol Microbiol 61:1239–1245. https://doi.org/10.1099/ijs.0.023663-0.
8. Lapaglia C, Hartzell PL. 1997. Stress-induced production of biofilm in the hyperthermophile *Archaeoglobus fulgidus*. Appl Environ Microbiol 63:3158–3163. https://doi.org/10.1128/aem.63.8.3158-3163.1997.
9. Jarrell KF, Stark M, Nair DB, Chong JPJ. 2011. Flagella and pili are both necessary for efficient attachment of *Methanococcus maripaludis* to surfaces. FEMS Microbiol Lett 319:44–50. https://doi.org/10.1111/j.1574-6968.2011.02264.x.
10. Brileya KA, Camilleri LB, Zane GM, Wall JD, Fields MW. 2014. Biofilm growth mode promotes maximum carrying capacity and community stability during product inhibition syntrophy. Front Microbiol 5:693. https://doi.org/10.3389/fmicb.2014.00693.
11. Uchiyama T, Ito K, Mori K, Tsurumaru H, Harayama S. 2010. Iron-corroding methanogen isolated from a crude-oil storage tank. Appl Environ Microbiol 76:1783–1788. https://doi.org/10.1128/AEM.00668-09.
12. Jarrell KF, Ding Y, Meyer BH, Albers S-V, Kaminski L, Eichler J. 2014. N-linked glycosylation in Archaea: a structural, functional, and genetic analysis. Microbiol Mol Biol Rev 78:304–341. https://doi.org/10.1128/MMBR.00052-13.

13. Chaban B, Voisin S, Kelly J, Logan SM, Jarrell KF. 2006. Identification of genes involved in the biosynthesis and attachment of *Methanococcus voltae* N-linked glycans: insight into N-linked glycosylation pathways in Archaea. Mol Microbiol 61:259–268. https://doi.org/10.1111/j.1365-2958.2006.05226.x.
14. Nair DB, Chung DKC, Schneider J, Uchida K, Aizawa S-I, Jarrell KF. 2013. Identification of an additional minor pilin essential for piliation in the archaeon *Methanococcus maripaludis*. PLoS One 8:e83961. https://doi.org/10.1371/journal.pone.0083961.
15. Ng SYM, Wu J, Nair DB, Logan SM, Robotham A, Tessier L, Kelly JF, Uchida K, Aizawa S-I, Jarrell KF. 2011. Genetic and mass spectrometry analyses of the unusual type IV-like pili of the archaeon *Methanococcus maripaludis*. J Bacteriol 193:804–814. https://doi.org/10.1128/JB.00822-10.
16. Jones GM, Wu J, Ding Y, Uchida K, Aizawa S-I, Robotham A, Logan SM, Kelly J, Jarrell KF. 2012. Identification of genes involved in the acetamidino group modification of the flagellin N-linked glycan of *Methanococcus maripaludis*. J Bacteriol 194:2693–2702. https://doi.org/10.1128/JB.06686-11.
17. Ding Y, Jones GM, Uchida K, Aizawa S-I, Robotham A, Logan SM, Kelly J, Jarrell KF. 2013. Identification of genes involved in the biosynthesis of the third and fourth sugars of the *Methanococcus maripaludis* archaellin N-linked tetrasaccharide. J Bacteriol 195:4094–4104. https://doi.org/10.1128/JB.00668-13.
18. Voisin S, Houliston RS, Kelly J, Brisson J-R, Watson D, Bardy SL, Jarrell KF, Logan SM. 2005. Identification and characterization of the unique N-linked glycan common to the flagellins and S-layer glycoprotein of *Methanococcus voltae*. J Biol Chem 280:16586–16593. https://doi.org/10.1074/jbc.M500329200.
19. Wang F, Cvirkaite-Krupovic V, Kreutzberger MAB, Su Z, de Oliveira GAP, Osinski T, Sherman N, DiMaio F, Wall JS, Prangishvili D, Krupovic M, Egelman EH. 2019. An extensively glycosylated archaeal pilus survives extreme conditions. Nat Microbiol 4:1401–1410. https://doi.org/10.1038/s41564-019-0458-x.
20. Wang F, Baquero DP, Su Z, Beltran LC, Prangishvili D, Krupovic M, Egelman EH. 2020. The structures of two archaeal type IV pili illuminate evolutionary relationships. Nat Commun 11:3424. https://doi.org/10.1038/s41467-020-17268-4.
21. Abu-Qarn M, Yurist-Doutsch S, Giordano A, Trauner A, Morris HR, Hitchen P, Medalia O, Dell A, Eichler J. 2007. *Haloferax volcanii* AglB and AglD are involved in N-glycosylation of the S-layer glycoprotein and proper assembly of the surface layer. J Mol Biol 374:1224–1236. https://doi.org/10.1016/j.jmb.2007.10.042.
22. Tripepi M, You J, Temel S, Önder Ö, Brisson D, Pohlschröder M. 2012. N-glycosylation of *Haloferax volcanii* flagellins requires known Agl proteins and is essential for biosynthesis of stable flagella. J Bacteriol 194:4876–4887. https://doi.org/10.1128/JB.00731-12.
23. Tripepi M, Imam S, Pohlschröder M. 2010. *Haloferax volcanii* flagella are required for motility but are not involved in PibD-dependent surface adhesion. J Bacteriol 192:3093–3102. https://doi.org/10.1128/JB.00133-10.
24. Shalev Y, Turgeman-Grott I, Tamir A, Eichler J, Gophna U. 2017. Cell surface glycosylation is required for efficient mating of *Haloferax volcanii*. Front Microbiol 8:1253. https://doi.org/10.3389/fmicb.2017.01253.
25. O'Toole GA. 2011. Microtiter dish biofilm formation assay. J Vis Exp 2011:2437. https://doi.org/10.3791/2437.
26. Merritt JH, Kadouri DE, O'Toole GA. 2005. Growing and analyzing static biofilms. Curr Protoc Microbiol Chapter 1:Unit 1B.1. https://doi.org/10.1002/9780471729259.mc01b01s00.
27. Ding Y, Vrionis HA, Schneider J, Berezuk A, Khursigara CM, Jarrell KF. 2016. Complementation of an *aglB* mutant of *Methanococcus maripaludis* with heterologous oligosaccharyltransferases. PLoS One 11:e0167611. https://doi.org/10.1371/journal.pone.0167611.
28. Ng SYM, Chaban B, Jarrell KF. 2006. Archaeal flagella, bacterial flagella and type IV pili: a comparison of genes and posttranslational modifications. J Mol Microbiol Biotechnol 11:167–191. https://doi.org/10.1159/000094053.
29. VanDyke DJ, Wu J, Logan SM, Kelly JF, Mizuno S, Aizawa S-I, Jarrell KF. 2009. Identification of genes involved in the assembly and attachment of a novel flagellin N-linked tetrasaccharide important for motility in the archaeon *Methanococcus maripaludis*. Mol Microbiol 72:633–644. https://doi.org/10.1111/j.1365-2958.2009.06671.x.
30. Goris J, Konstantinidis KT, Klappenbach JA, Coenye T, Vandamme P, Tiedje JM. 2007. DNA-DNA hybridization values and their relationship to whole-genome sequence similarities. Int J Syst Evol Microbiol 57:81–91. https://doi.org/10.1099/ijs.0.64483-0.
31. Rodriguez-R LM, Konstantinidis KT. 2016. The enveomics collection: a toolbox for specialized analyses of microbial genomes and metagenomes. PeerJ Preprints 4:e1900v1. https://peerj.com/preprints/1900/.
32. Poehlein A, Heym D, Quitzke V, Fersch J, Daniel R, Rother M. 2018. Complete genome sequence of the *Methanococcus maripaludis* type strain JJ (DSM 2067), a model for selenoprotein synthesis in Archaea. Genome Announc 6:e00237-18. https://doi.org/10.1128/genomeA.00237-18.
33. Hendrickson EL, Kaul R, Zhou Y, Bovee D, Chapman P, Chung J, Conway de Macario E, Dodsworth JA, Gillett W, Graham DE, Hackett M, Haydock AK, Kang A, Land ML, Levy R, Lie TJ, Major TA, Moore BC, Porat I, Palmeiri A, Rouse G, Saenphimmachak C, Söll D, Van Dien S, Wang T, Whitman WB, Xia Q, Zhang Y, Larimer FW, Olson MV, Leigh JA. 2004. Complete genome sequence of the genetically tractable hydrogenotrophic methanogen *Methanococcus maripaludis*. J Bacteriol 186:6956–6969. https://doi.org/10.1128/JB.186.20.6956-6969.2004.
34. Fonseca DR, Abdul Halim MF, Holten MP, Costa KC. 2020. Type IV pili facilitate transformation in naturally competent archaea. J Bacteriol 202:e00355-20. https://doi.org/10.1128/JB.00355-20.
35. Tumbula DL, Makula RA, Whitman WB. 1994. Transformation of *Methanococcus maripaludis* and identification of a *Pst* I-like restriction system. FEMS Microbiol Lett 121:309–314. https://doi.org/10.1111/j.1574-6968.1994.tb07118.x.
36. Sarmiento FB, Leigh JA, Whitman WB. 2011. Genetic systems for hydrogenotrophic methanogens. Methods Enzymol 494:43–73. https://doi.org/10.1016/B978-0-12-385112-3.00003-2.
37. Doerner KC, White BA. 1990. Detection of glycoproteins separated by nondenaturing polyacrylamide gel electrophoresis using the periodic acid-Schiff stain. Anal Biochem 187:147–150. https://doi.org/10.1016/0003-2697(90)90433-A.
38. Moravec J, Mares J. 2017. A simple, time-saving, microwave-assisted periodic acid-Schiff˙s staining of glycoproteins on 1D electrophoretic gels. Electrophoresis 38:3100–3103. https://doi.org/10.1002/elps.201700189.
39. Tsurumaru H, Ito N, Mori K, Wakai S, Uchiyama T, Iino T, Hosoyama A, Ataku H, Nishijima K, Mise M, Shimizu A, Harada T, Horikawa H, Ichikawa N, Sekigawa T, Jinno K, Tanikawa S, Yamazaki J, Sasaki K, Yamazaki S, Fujita N, Harayama S. 2018. An extracellular [NiFe] hydrogenase mediating iron corrosion is encoded in a genetically unstable genomic island in *Methanococcus maripaludis*. Sci Rep 8:15149. https://doi.org/10.1038/s41598-018-33541-5.
40. Lahme S, Mand J, Longwell J, Smith R, Enning D. 2021. Severe corrosion of carbon steel in oil field produced water can be linked to methanogenic archaea containing a special type of [nife] hydrogenase. Appl Environ Microbiol 87:e01819-20. https://doi.org/10.1128/AEM.01819-20.
41. Brileya KA, Connolly JM, Downey C, Gerlach R, Fields MW. 2013. Taxis toward hydrogen gas by *Methanococcus maripaludis*. Sci Rep 3:3140. https://doi.org/10.1038/srep03140.
42. Thennarasu S, Polireddy D, Antony A, Yada MR, Algarawi S, Sivakumar N. 2013. Draft genome sequence of a highly flagellated, fast-swimming archaeon, *Methanocaldococcus villosus* strain KIN24-T80 (DSM 22612). Genome Announc 1:e00481-13. https://doi.org/10.1128/genomeA.00481-13.
43. König H, Kralik R, Kandler O. 1982. Structure and modifications of pseudomurein in Methanobacleriales. Zentralbl Bakteriol Mikrobiol Hyg I Abt Orig C 3:179–191. https://doi.org/10.1016/S0721-9571(82)80031-8.
44. Ishii S, Kosaka T, Hori K, Hotta Y, Watanabe K. 2005. Coaggregation facilitates interspecies hydrogen transfer between *Pelotomaculum thermopropionicum* and *Methanothermobacter thermautotrophicus*. Appl Environ Microbiol 71:7838–7845. https://doi.org/10.1128/AEM.71.12.7838-7845.2005.
45. Costa KC, Wong PM, Wang T, Lie TJ, Dodsworth JA, Swanson I, Burn JA, Hackett M, Leigh JA. 2010. Protein complexing in a methanogen suggests electron bifurcation and electron delivery from formate to heterodisulfide reductase. Proc Natl Acad Sci U S A 107:11050–11055. https://doi.org/10.1073/pnas.1003653107.
46. Koerdt A, Gödeke J, Berger J, Thormann KM, Albers S-V. 2010. Crenarchaeal biofilm formation under extreme conditions. PLoS One 5:e14104. https://doi.org/10.1371/journal.pone.0014104.
47. Legerme G, Yang E, Esquivel RN, Kiljunen S, Savilahti H, Pohlschroder M. 2016. Screening of a *Haloferax volcanii* transposon library reveals novel motility and adhesion mutants. Life 6:41. https://doi.org/10.3390/life6040041.
48. Rollefson JB, Levar CE, Bond DR. 2009. Identification of genes involved in biofilm formation and respiration via mini-Himar transposon mutagenesis of *Geobacter sulfurreducens*. J Bacteriol 191:4207–4217. https://doi.org/10.1128/JB.00057-09.

49. Levar CE, Chan CH, Mehta-Kolte MG, Bond DR. 2014. An inner membrane cytochrome required only for reduction of high redox potential extracellular electron acceptors. mBio 5:e02034-14. https://doi.org/10.1128/mBio.02034-14.
50. Gibson DG, Young L, Chuang R-Y, Venter JC, Hutchison CA, Smith HO. 2009. Enzymatic assembly of DNA molecules up to several hundred kilobases. Nat Methods 6:343–345. https://doi.org/10.1038/nmeth.1318.
51. Dodsworth JA, Leigh JA. 2006. Regulation of nitrogenase by 2-oxoglutarate-reversible, direct binding of a PII-like nitrogen sensor protein to dinitrogenase. Proc Natl Acad Sci U S A 103:9779–9784. https://doi.org/10.1073/pnas.0602278103.
52. Whitman WB, Shieh J, Sohn S, Caras DS, Premachandran U. 1986. Isolation and characterization of 22 mesophilic methanococci. Syst Appl Microbiol 7:235–240. https://doi.org/10.1016/S0723-2020(86)80012-1.
53. Jones WJ, Paynter MJB, Gupta R. 1983. Characterization of *Methanococcus maripaludis* sp. nov., a new methanogen isolated from salt marsh sediment. Arch Microbiol 135:91–97. https://doi.org/10.1007/BF00408015.